A Conformational Change in Heparan Sulfate 3-*O*-Sulfotransferase-1 Is Induced by Binding to Heparan Sulfate†

Suzanne C. Edavettal,‡ Kevin Carrick,§ Ruchir R. Shah,|| Lars C. Pedersen,⊥ Alexander Tropsha,‡,|| R. Marshall Pope,§ and Jian Liu*,‡

Division of Medicinal Chemistry and Natural Products, School of Pharmacy, Proteomic Core Facility, Department of Biochemistry, and Laboratory of Molecular Modeling, School of Pharmacy, University of North Carolina, Chapel Hill, North Carolina 27599, and Laboratory of Structural Biology, National Institute of Environmental Health Sciences, National Institutes of Health, Research Triangle Park, North Carolina 27709

Received January 12, 2004; Revised Manuscript Received February 24, 2004

ABSTRACT: The 3-*O*-sulfation of glucosamine by heparan sulfate 3-*O*-sulfotransferase-1 (3-OST-1) is a key modification step during the biosynthesis of anticoagulant heparan sulfate (HS). In this paper, we present evidence of a conformational change that occurs in 3-OST-1 upon binding to heparan sulfate. The intrinsic fluorescence of 3-OST-1 was increased in the presence of HS, suggesting a conformational change. This apparent conformational change was further investigated using differential chemical modification of 3-OST-1 to measure the solvent accessibility of the lysine residues. 3-OST-1 was treated with acetic anhydride in either the presence or absence of HS using both acetic anhydride and hexadeuterioacetic anhydride under nondenaturing and denaturing conditions, respectively. The relative reactivity of the lysine residues to acetylation and [^{2}H] acetylation in the presence or absence of HS was analyzed by measuring the ratio of acetylated and deuterioacetylated peptides using matrix-assisted laser desorption ionization mass spectrometry. The solvent accessibilities of the lysine residues were altered differentially depending on their location. In particular, we observed a group of lysine residues in the C-terminus of 3-OST-1 that become more solvent accessible when 3-OST-1 binds to HS. This observation indicates that a conformational change could be occurring during substrate binding. A truncated mutant of 3-OST-1 that lacked this C-terminal region was expressed and found to exhibit a 200-fold reduction in sulfotransferase activity. The results from this study will contribute to our understanding of the interactions between 3-OSTs and HS.

Heparan sulfate proteoglycans (HSPGs) are present in large quantities on the surface of most mammalian cells and in the extracellular matrix. HSPGs are comprised of core proteins and highly sulfated polysaccharide chains. Heparan sulfate (HS)[1] is a structurally complex polysaccharide comprised of repeating 1−4-linked sulfated glucosamine and sulfated glucuronic/iduronic acid disaccharides. The functions of HSPGs are largely determined by their HS polysaccharide side chains. HS plays critical roles in a variety of biological processes, including assisting viral infection, regulating blood coagulation and embryonic development, suppressing tumor growth, and controlling the eating behavior of mice by interacting with specific regulatory proteins (*1*−*5*). The specific sulfated saccharide sequences within HS determine the specificity of binding to proteins (*6*).

Specific sulfated saccharide sequences are introduced into the HS chain during biosynthesis. HS is initially synthesized as a copolymer of glucuronic acid and *N*-acetylated glucosamine by D-glucuronyl- and *N*-acetyl-D-glucosaminyltransferase. Following polymerization, various modifications, including sulfation and epimerization, occur to HS in the Golgi apparatus (*7*). C_5 epimerization of glucuronic acid to iduronic acid is catalyzed by glucuronyl C_5 epimerase. *N*-Deacetylase/*N*-sulfotransferase (NDST) catalyzes *N*-deacetylation/*N*-sulfation of glucosamine residues. 2-*O*-Sulfation of iduronic and glucuronic acid residues and 6-*O*-sulfation and 3-*O*-sulfation of glucosamine residues are catalyzed by the uronyl 2-*O*-sulfotransferase (2-OST) and glucosaminyl

† This work is supported in part by a grant from the National Institutes of Health (AI50050, to J.L.) and a grant from American Heart Association Mid-Atlantic Affiliate (0355800U, to J.L.).

* To whom correspondence should be addressed: Room 309, Beard Hall, School of Pharmacy, University of North Carolina, Chapel Hill, NC 27599. Phone: (919) 843-6511. Fax: (919) 843-5432. E-mail: jian_liu@unc.edu.

‡ Division of Medicinal Chemistry and Natural Products, School of Pharmacy, University of North Carolina.

§ Proteomic Core Facility, Department of Biochemistry, University of North Carolina.

|| Laboratory of Molecular Modeling, School of Pharmacy, University of North Carolina.

⊥ National Institutes of Health.

[1] Abbreviations: 3-OST-1, 3-OST-3A, and 3-OST-5, heparan sulfate 3-*O*-sulfotransferase isoforms 1, 3A, and 5, respectively; HS, heparan sulfate; NDST, heparan sulfate *N*-deacetylase/*N*-sulfotransferase; AT, antithrombin; HSV-1 gD, herpes simplex virus-1 glycoprotein D; PAP, 3′-phosphoadenosine 5′-phosphate or 3′,5′-adenosine diphosphate; PAPS, 3′-phosphoadenosine 5′-phosphosulfate; MOPS, 3-(*N*-morpholino)propanesulfonic acid; CS, chondroitin sulfate; MALDI-TOF MS, matrix-assisted laser desorption ionization time-of-flight mass spectrometry; b3-OST-1, mouse 3-OST-1 expressed in *Escherichia coli*; truncated b3-OST-1, mouse 3-OST-1 expressed in *E. coli* with C-terminal truncation of 28 amino acids; λ_{em}, maximum emission wavelength; λ_{ex}, excitation wavelength.

10.1021/bi0499112 CCC: $27.50
Published on Web 04/02/2004

6-*O*- and 3-*O*-sulfotransfease (6-OST and 3-OST, respectively), respectively.

HS sulfotransferases, except for 2-OST, are present in multiple isoforms, and these isoforms have tissue specific expression patterns (*8*−*11*). The expression levels of these isoforms could play roles in regulating the biosynthesis of the HS with defined saccharide sequences. NDST and 3-OST isoforms recognize the saccharide sequences around the modification sites which exhibit different substrate specificities (*8*, *11*, *12*), whereas distinct substrate specificities among 6-OST isoforms were not detected (*13*, *14*).

Six different 3-OST isoforms have been identified (*10*, *12*). The 3-*O*-sulfation of glucosamine represents the final modification step during the biosynthesis of biologically active HS. 3-*O*-sulfated HS is known to bind to antithrombin (AT), herpes simplex virus-1 glycoprotein D (HSV-1 gD), and growth factor receptor and fibroblast growth factor 7 (*15*−*18*). In addition, 3-*O*-sulfated HS has been implicated in regulation of circadian rhythms (*19*) and various human cancers (*20*). The diverse biological functions of 3-*O*-sulfated HS are likely biosynthesized by different 3-OST isoforms. In fact, 3-OST isoform 1 (3-OST-1) and 3-OST-5 are responsible for key modifications in the biosynthesis of HS that binds AT (*12*, *15*). 3-OST-3 and 3-OST-5 are known to introduce key 3-*O*-sulfated groups during the biosynthesis of HS that bind HSV-1 gD (*12*, *17*).

The mechanism that HS sulfotransferases use to recognize their substrates is unknown. The crystal structure of the binary complex of NDST and 3′-phosphoadenosine 5′-phosphate (PAP) was determined by Kakuta and colleagues (*21*). On the basis of the crystal structure, a computer model of the ternary complex of NDST, PAPS (3′-phosphoadenosine 5′-phosphosulfate), and a disaccharide substrate was published (*22*). In addition, a homology model of human 3-OST-1 that used the NDST structure as a template has been reported (*23*). The results from these studies suggest that the sulfotransferase reaction mechanisms of NDST and 3-OST-1 are very similar to that of estrogen sulfotransferase (*24*). However, the actual substrate recognition mechanism for NDST and 3-OST-1 is unknown. Our research has been focused on understanding the substrate recognition mechanism for 3-OSTs. Although the sequences of 3-OST isoforms are more than 60% homologous in the sulfotransferase domain, the substrate specificities are remarkably distinct. In this article, we describe a conformational change occurring in 3-OST-1 upon binding to HS. The conformational change was detected by observing an increase in the intrinsic fluorescence of 3-OST-1 and a difference in the reactivity to acetylation in the presence or absence of HS. The observation of the conformational change contributes to our understanding of the interactions between 3-OSTs and HS.

EXPERIMENTAL PROCEDURES

Materials. Recombinant mouse 3-OST-1 (m3-OST-1), human 3-OST-3A (h3-OST-3), and human 3-OST-5 (h3-OST-5) enzymes were expressed in Sf9 cells using a baculovirus expression system. The enzymes were purified by heparin−Toyopearl and 3′,5′-ADP−agarose chromatographies as described previously (*25*, *26*). [^{35}S]PAPS was prepared by incubating 0.4−2 mCi/mL [^{35}S]Na_2SO_4 (carrier-free, ICN) and 16 mM ATP with 5 mg/mL dialyzed yeast extract (Sigma) (*15*). HS from bovine kidney and chondroitin sulfate C (CS) were purchased from ICN and Sigma, respectively.

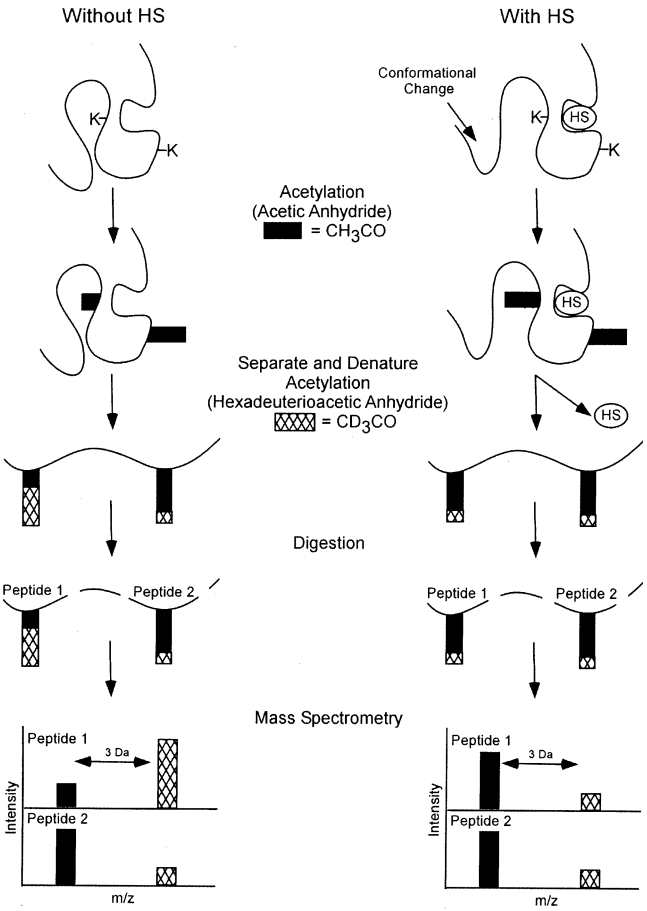

FIGURE 1: Scheme for differential chemical acetylation of lysine residues of m3-OST-1 [adapted from Hochleitner *et al.* (*27*)].

Determination of the Intrinsic Fluorescence of 3-OSTs. The intrinsic fluorescence of 3-OSTs was measured using approximately 125 nM 3-OST in buffer containing 100 mM 3-(*N*-morpholino)propanesulfonic acid (MOPS, Sigma) (pH 7.0), 10 mM $MgCl_2$, 5 mM $MnCl_2$, 60 μM Zwittergent 3-16 (CalBioChem), 2% glycerol, and 30 μM 3′,5′-adenosine diphosphate (PAP, Sigma), at 25 °C with spectral bandwidths of 4 nm (excitation) and 16 nm (emission). Using an excitation wavelength of 295 nm, an emission scan was preformed from 310 to 430 nm, with a maximum emission wavelength observed at 330 nm. Spectra were also collected after addition of HS or CS (10 μM) and a brief mixing. The percent change was calculated as the difference in the fluorescence intensity at 330 nm between the samples with HS or CS and without HS or CS.

Differential Chemical Modification. The differential chemical modification protocol described below was adapted from Hochleitner *et al.* (*27*) and is illustrated in Figure 1. Approximately 10 μg of m3-OST-1 was subjected to acetylation under nondenaturing conditions using 100 μM acetic anhydride in a buffer containing 100 mM MOPS (pH 7.0), 10 mM $MgCl_2$, 5 mM $MnCl_2$, 60 μM Zwittergent 3-16, 2% glycerol, 50 mM NaCl, and 30 μM PAP (buffer 1) at 4 °C, in solution (acetylation without HS). The reaction was allowed to proceed for 30 min and quenched with the addition of 50 mM Tris (pH 7.0), and then the mixture was

dialyzed against buffer containing 1 M NaCl, 100 mM MOPS (pH 7.0), 60 μM Zwittergent 3-16, and 2% glycerol. The pH was monitored and remained neutral throughout the course of the acetylation.

To perform the acetylation with HS, the reaction was performed using an on-column format. Approximately 10 μg of m3-OST-1 was loaded on a 0.25 mL heparin−Sepharose column which had been pre-equilibrated with buffer 1 at 4 °C. One milliliter of buffer 1 and 100 μM acetic anhydride was passed over the column at a flow rate of 0.1 mL/min. The reaction was quenched with 0.25 mL of 1 M Tris (pH 7.0) at a flow rate of 0.1 mL/min, and the column was washed with 0.5 mL of buffer 1. The on-column acetylation was repeated once, and the protein was eluted with buffer containing 1 M NaCl, 100 mM MOPS (pH 7.0), 60 μM Zwittergent 3-16, and 2% glycerol.

Both samples (with and without HS) were then subjected to acetylation under denaturing conditions. The samples were incubated at 100 °C for 5 min, allowed to cool to 4 °C, and then subjected to complete acetylation using 1.2 mM hexadeuterioacetic anhydride ([^{2}H]acetic anhydride, Aldrich) in 80 mM Na_2CO_3 (pH 11) for 30 min at 4 °C. After that, additional 1.2 mM [^{2}H]acetic anhydride in 80 mM Na_2CO_3 (pH 11) was added; the mixture was allowed to incubate for an additional 30 min at 4 °C, and then the reaction was quenched with 50 mM Tris (pH 7.0). The protein samples were resolved on a precast 16.5% Tris-Tricine SDS−PAGE gel (Bio-Rad), and the gel was stained with Coomassie blue. The acetylated protein migrated as one band at approximately 37 kDa. The bands were cut from the gel and subjected to in-gel trypsin digestion with a Genomics Solutions ProGest robot using trypsin in 50 mM ammonium bicarbonate (pH 8) (*28*). The resultant peptides were analyzed using matrix-assisted desorption ionization time-of-flight mass spectrometry (MALDI-TOF MS).

MALDI-TOF MS was performed with a Bruker Reflex III TOF mass spectrometer. Extracted peptides were lyophilized and reconstituted in 5 μL of 50% methanol (v/v) and 0.1% formic acid. Peptides (0.5 μL) were then mixed with 1 μL of saturated α-cyanohydroxycinnamic acid in a 50% acetonitrile/0.1% trifluoroacetic acid mixture, placed on a target plate, and allowed to dry at 25 °C. For acetylated peptide identification, Bruker BioTools SequenceEditor software was used to match the molecular mass of peptides against the m3-OST-1 amino acid sequence (GenBank accession number AF019385). The relative reactivity of each lysine residue with respect to acetic anhydride (protonated and deuterated) was calculated from the integrated intensity of each identified signal [relative reactivity = trideuterioacetylated lysine/(trideuterioacetylated lysine + acetylated lysine) × 100].

Expression of m3-OST-1 and m3-OST-1(K284STP) in Escherichia coli. An *Nde*I site was introduced into the m3-OST-1 pcDNA3 vector (*29*) using polymerase chain reaction (PCR) upstream of m3-OST-1 amino acid position Gly48. This construct was inserted into the pET-28a vector (Novagen) using *Nde*I and *Eco*RI, and the resultant encoded m3-OST-1 with an N-terminal truncation of 47 amino acids (b3-OST-1). The plasmid was sequenced to confirm the reading frame (at the University of North Carolina DNA Sequencing Core Facility) and transformed into BL21-DE3 cells (Novegen). A 2 L LB culture (containing 50 μg/mL kanamycin) was inoculated and allowed to grow at 37 °C until the OD_{600} reached 0.8. The cultures were then cooled to 22 °C, and expression was induced by addition of 200 μg/mL isopropyl β-D-thiogalactopyranoside (IPTG, Promega). The cultures continued to grow overnight at 22 °C with constant shaking. The cells were harvested by centrifugation at 4500*g* for 20 min. The resultant cell pellet was resuspended in 40 mL of a buffer containing 25 mM Tris (pH 7.5), 500 mM NaCl, and 10 mM imidazole (buffer A). The cells were lysed using sonication, and the soluble fraction was isolated by centrifugation at 10000*g* for 30 min at 4 °C and filtration through a 0.2 μm filter.

Nickel chromatography was used to purify b3-OST- 1 as the protein contains a $(His)_6$ tag at the N-terminus. The bacterial lysate was loaded on an NTA−agarose (Qiagen) column (12 mm × 88 mm), which had been pre-equilibrated with buffer A at a flow rate of 3 mL/min. Unbound material was removed by extensive washing with buffer A, and the bound proteins were eluted with a linear gradient of imidazole from 10 to 250 mM over the course of 33.3 min. The b3-OST-1 emerged between 100 and 200 mM imidazole. b3-OST-1 has a substrate specificity identical to that of m3-OST-1 that was expressed in insect cells (data not shown).

A truncated b3-OST-1 mutant, which lacked the 28 C-terminal amino acids (truncated b3-OST-1), was constructed using the Gene Tailor site-directed mutagenesis kit from Invitrogen. The C-terminal truncation was achieved by introducing a K284STP mutation in the b3-OST-1 pET-28a cDNA by PCR [using the primers 5′-CACCCCCAGGTGGATCCC**T**AACTACTTGATA-3′ and 5′-GGGATCCACCTGGGGGTGCGCCCGGCCT-3′ (the point mutation is bold)]. The resultant construct was sequenced to confirm the mutation (University of North Carolina DNA Sequencing Core Facility). The mutant was expressed and purified in the manner described above for b3-OST-1.

Measurement of Sulfotransferase Activity. Sulfotransferase activity was determined by incubating approximately 35 ng of purified protein with 10 μg of HS (from bovine kidney, ICN) and 5 × 10^6 cpm of [^{35}S]PAPS (∼400 μM) in 50 μL of a buffer containing 50 mM MOPS (pH 7.0), 10 mM $MnCl_2$, 5 mM $MgCl_2$, and 1% Triton X-100. The reaction mixture was incubated at 37 °C for 90 min, and the reaction was quenched by addition of 6 M urea and 100 mM EDTA. The sample was then subjected to DEAE-Sepharose (200 μL) chromatography to purify the [^{35}S]HS. The quantity of [^{35}S]HS was then determined by scintillation counting.

Determination of the Level of Binding of b3-OST-1 and Truncated b3-OST-1 to PAP and Heparin. To determine the binding affinity of the wild-type and truncated b3-OST-1 for PAPS, 3′,5′-ADP−agarose chromatography (Sigma) was used. Approximately 200 μg of protein in 5 mL of a buffer containing 25 mM Tris (pH 7.0) and 100 mM NaCl was loaded onto a 3′,5′-ADP−agarose column (7 mm × 52 mm) which had been pre-equilibrated with 25 mM Tris (pH 7.0) and 100 mM NaCl at a flow rate of 0.5 mL/min. Unbound material was removed and collected with 5 mL of 25 mM Tris (pH 7.0) and 100 mM NaCl. The bound proteins were eluted with 5 mL of a buffer containing 25 mM Tris (pH 7.0) and 250 mM NaCl (low-ionic strength elution fraction) and 1 mL of a buffer containing 25 mM Tris (pH 7.0) and 1 M NaCl (high-ionic strength elution fraction). The samples from each eluted fraction were analyzed by SDS−PAGE, and the gel was stained with Coomassie blue.

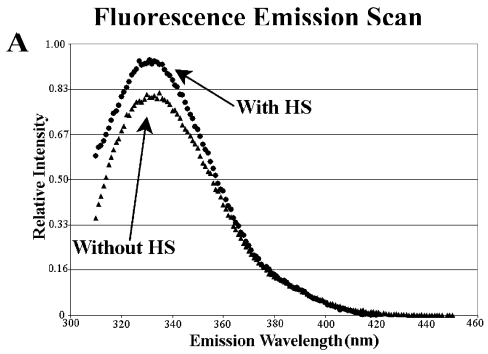

B

Percent Change in Fluorescence at λ_{EM} = 330 nm)

	+HS	+CS
m3-OST-1	14%±0.3% (n = 4)	-0.4±0.2% (n = 2)
h3-OST-3	27%±7% (n = 2)	7%±3% (n = 2)
h3-OST-5	29%±9% (n = 2)	-8%±0.4% (n = 2)

FIGURE 2: Increase in the intrinsic fluorescence of 3-OSTs upon binding to HS. Using a λ_{ex} of 295 nm, a fluorescence emission scan of 3-OSTs over a λ_{em} range of 310−430 nm was completed with and without HS and CS. An emission scan of 3-OST-1 with and without HS is shown in panel A: without HS (▲) and with HS (●). The difference in maximum intensity (λ_{em} = 330 nm) was used to calculate the percent change [percent change = (with ligand − without ligand)/without ligand] shown in panel B.

To determine the affinity of wild-type and mutant m3-OST-1 for HS, heparin−Sepharose chromatography (Pharmacia) was used. Approximately 200 μg of protein in 5 mL of a buffer containing 25 mM Tris (pH 7.0) and 100 mM NaCl was loaded onto a heparin−Sepharose column (7 mm × 52 mm), which had been pre-equilibrated with a buffer containing 25 mM Tris (pH 7.0) and 100 mM NaCl. Unbound material was removed and collected with 5 mL of a buffer containing 25 mM Tris (pH 7.0) and 100 mM NaCl. The bound proteins were eluted with 5 mL of a buffer containing 25 mM Tris (pH 7.0) and 250 mM NaCl (low-ionic strength elution fraction) and 1 mL of a buffer containing 25 mM Tris (pH 7.0) and 1 M NaCl (high-ionic strength elution fraction). The samples from each eluted fraction were analyzed by SDS−PAGE, and the gel was stained with Coomassie blue.

Homology Model of m3-OST-1. m3-OST-1 was homology modeled using the crystal structure of the sulfotransferase domain of human NDST-1 [PDB entry 1NST (*21*)] as the template structure. To select a template protein structure for modeling the m3-OST-1 structure, we used the primary m3-OST-1 protein sequence and aligned it with all proteins in the Protein Data Bank. The sequence alignment was performed on the Biology workbench (http://workbench.sdsc.edu/) using the BLAST sequence alignment tool with the BLOSUM62 substitution matrix, affine gap penalties (gap opening penalty of −11, gap extension penalty of −1), and a Lambda ratio of 0.85. Hits were ranked by their *e* values. NDST-1 had the lowest *e* value of all matched proteins (*e* value = 9×10^{-24}) with a sequence approximately 30% identical with that of m3-OST-1. The PAP binding domains were constrained during modeling as described by Raman *et al*. (*23*). The model had a score of 86 when verified using profiles_3D, where a score of 115 would be expected for a valid protein of the same size. The model was created using the homology modeling module of Insight-II.

RESULTS

Heparan Sulfate Increases the Intensity of the Intrinsic Fluorescence of 3-OSTs. The intrinsic fluorescence was measured for m3-OST-1, h3-OST-3A, and h3-OST-5. The maximum emission wavelength (λ_{em}) was observed for all proteins at 330 nm, using an excitation wavelength (λ_{ex}) of 295 nm. The percent change was calculated as the difference in the fluorescence intensity between the samples with HS or CS and without HS or CS at λ_{em}. Incubation of HS with 3-OSTs induced an increase in the intensity of the intrinsic fluorescence for all proteins at λ_{em} (14% m3-OST-1, 27% h3-OST-3, and 29% for h3-OST-5), with no shift in λ_{em} observed (Figure 2). To demonstrate that the change in the observed fluorescence intensity was due to binding of the enzyme to its substrate (HS), we incubated the 3-OSTs with CS, which is not a substrate for any of the 3-OSTs (*15*, *25*, *26*). Incubation of CS with 3-OST-3 induced a 7% increase in fluorescence intensity, which is ∼4-fold less than that of the incubation with HS. Furthermore, an unchanged or decreased fluorescence intensity was observed when 3-OST-1 or 3-OST-5 was incubated with CS, respectively. These data indicate that the increase in fluorescence intensity is due to a specific interaction between 3-OSTs and HS.

Differential Chemical Modification. The increase in the intensity of the intrinsic protein fluorescence was observed when 3-OSTs were bound to HS, suggesting that a conformational change occurs when the sulfotransferases interact with the substrate. To gain additional information concerning any possible conformational changes that may occur in m3-OST-1 upon HS binding, we determined the relative susceptibility of lysine residues to acetylation by acetic anhydride. This approach has been used with several different proteins, including human immunodeficiency virus core protein p24 (*27*), lysozyme (*30*), and human catechol *O*-methyltransferase (*31*), to determine the solvent accessibility of lysine residues. Figure 1 illustrates the approach used to differentially acetylate the lysine residues of m3-OST-1 with and without HS bound. First, acetylation of the lysine residues of 3-OST-1 with and without HS bound was carried out using acetic anhydride under nondenaturing conditions. After the initial acetylation, a more complete acetylation was carried out using hexadeuterioacetic anhydride ([^{2}H]acetic anhydride) under denaturing conditions. The acetylated proteins were resolved on SDS−PAGE, and the protein was subjected to in-gel digestion with trypsin. MALDI MS was employed to determine the ratio of resultant peptides containing acetylated (protonated) lysine and ^{2}H-labeled acetylated (trideuterated) lysine residues. The MALDI MS spectra for m3-OST-1 with and without bound HS are shown in Figure 3. The inset illustrates the expanded spectra for the acetylated and ^{2}H-labeled acetylated lysine residues. The relative reactivity of each lysine residue was calculated from the abundance of each identified signal [relative

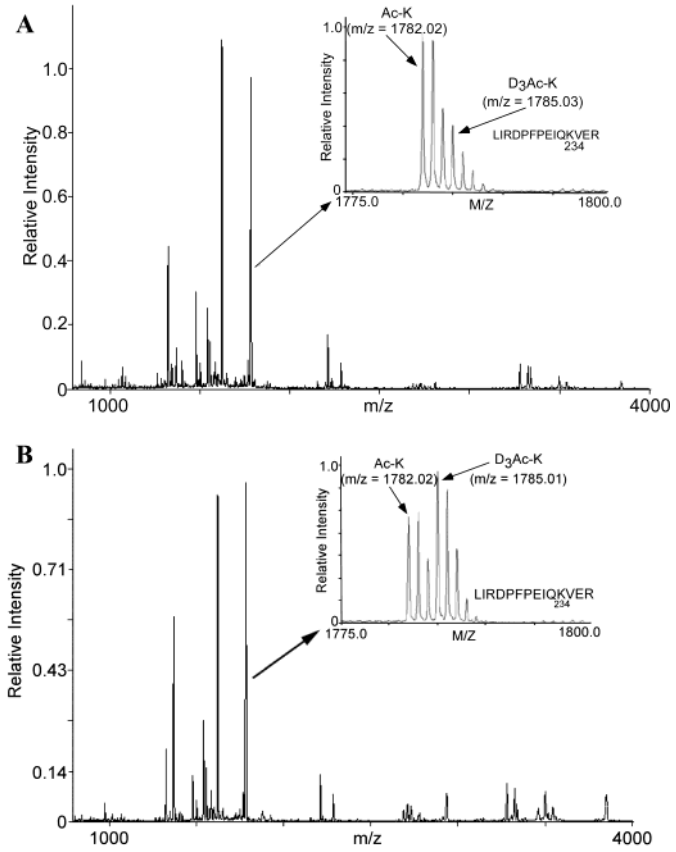

FIGURE 3: MALDI-TOF mass spectra of m3-OST-1 that had been chemically modified with HS bound and without HS bound. Panel A shows the mass spectrum of the protonated tryptic peptides from 3-OST-1 chemically modified in the presence of HS. The inset is an expanded spectrum of the peak at *m*/*z* 1782.02 to demonstrate the acetylated (Ac-K) and trideuterioacetylated peptides (D_3Ac-K). Panel B shows the mass spectrum of the protonated tryptic peptides from 3-OST-1 chemically modified in the absence of HS. The inset is an expanded spectrum of the peak at *m*/*z* 1782.02 to demonstrate the acetylated (Ac-K) and trideuterioacetylated peptides (D_3Ac-K).

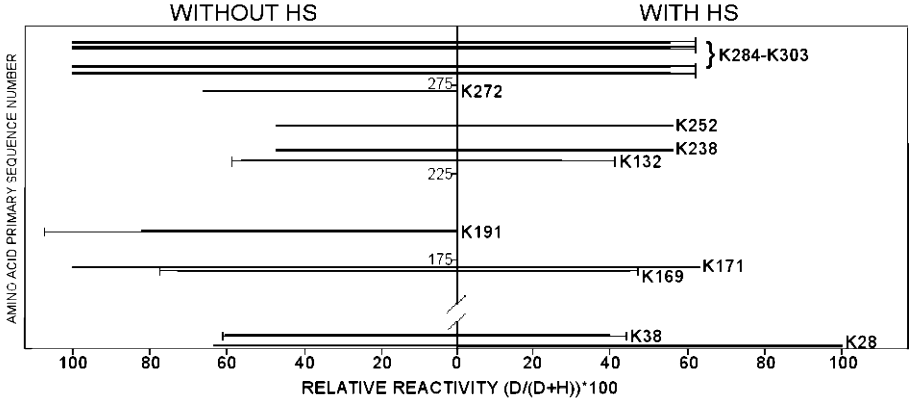

FIGURE 4: Relative reactivity of chemically modified lysine residues from m3-OST-1. The relative reactivity was calculated from the intensity of each MS peak [relative reactivity = trideuterioacetylated lysine/(trideuterioacetylated lysine + acetylated lysine) × 100]. Columns represent the mean of two independent experiments. Error bars represent the range.

reactivity = (^{2}H-labeled acetylated lysine/(^{2}H-labeled acetylated lysine + acetylated lysine) × 100] (Figure 4).

We next compared the percentage of the identical ^{2}H-labeled acetylated peptides of 3-OST-1. We observed that lysine residues in different regions of m3-OST-1 have distinct relative reactivity with respect to acetylation in the presence or absence of HS (Figure 4). These results suggest that the solvent accessibility of the lysine residues is altered differentially when the enzyme interacts with HS. The higher percentage of ^{2}H-labeled acetylated peptide suggests lower solvent accessibility in a nondenaturing buffer, such as a biological buffer. As expected, certain lysine residues were observed to have little or moderate differences in relative reactivity with respect to acetic anhydride. For example, K252 was observed to have relative reactivities of 56 and 47% in the presence and absence of HS, respectively, suggesting that the solvent accessibility of K252 is independent of HS binding. However, K28 was observed to have a greater relative reactivity with HS bound than without (100 and 64%, respectively), suggesting that K28 is less solvent accessible when the enzyme binds HS. Conversely, a stretch of lysine residues (K284, K289, K299, K300, and K303) in the C-terminal domain exhibits a lower relative reactivity when the enzyme binds HS. We observed that the percent-

Table 1: Sulfotransferase Activities of b3-OST-1 and the Truncated b3-OST-1

protein	pmol of [^{35}S]sulfate transferred/μg of protein
b3-OST-1	6.4
truncated b3-OST-1	0.032 ± 0.009

ages of ^{2}H-labeled acetylated lysine residues are nearly 2-fold lower in the presence of HS than in the absence of HS, suggesting that this region becomes substantially more solvent accessible when the enzyme binds HS. Because we observed that the relative reactivity of the lysine residues in numerous regions of the enzyme was altered upon binding to HS, the results are consistent with the conclusion that a conformational change occurs in m3-OST-1 upon binding to HS.

The C-Terminus Is Required for Sulfotransferase Activity. The C-terminal region has attracted our attention as this region undergoes substantial conformational changes when the enzyme binds to HS. In addition, the function of this region has not been reported previously, and it does not include the proposed HS binding or PAPS binding domains (*23*, *32*). To explore the role of this C-terminal region in the function of 3-OST-1, we prepared a point mutant protein (K284STP) which lacked the C-terminal region (truncated b3-OST-1) from residue 284 to 307. The mutant protein was expressed at levels approximately 5-fold lower than that of the wild-type enzyme; however, we were able to purify a small amount. The truncated b3-OST-1 exhibited approximately a 200-fold decrease in sulfotransferase activity, as compared with b3-OST-1 (Table 1). These data suggest that this C-terminal domain is critically important for sulfotransferase activity. Intrinsic protein fluorescence experiments were also completed with the truncated b3-OST-1. The truncated mutant was observed to have a $4.9 \pm 0.3\%$ increase in fluorescence at λ_{em} upon the addition of HS; however, a similar increase in fluorescence was also observed upon addition of CS, suggesting that the fluorescence increase of truncated b3-OST-1 is not due to the specific binding of substrate. The lack of the substrate-induced increase in the intrinsic fluorescence for truncated b3-OST-1 suggests that the fluorescence increase is associated with sulfotransferase activity.

To further characterize the truncated b3-OST-1, HS and PAPS binding experiments were conducted. Because of the low sulfotransferase activity of the truncated b3-OST-1, kinetic analysis could not be completed to determine the K_m values for HS and PAPS. In addition, we were unable to purify truncated b3-OST-1 in relatively large quantities; thus, a direct measurement of the binding affinity between truncated b3-OST-1 and HS or PAPS was difficult. To overcome these difficulties, affinity chromatography was employed as described in the study of flavonol 3-*O*-sulfotransferase (*33*). Heparin−Sepharose chromatography was used to determine HS binding affinity, and 3′,5′-ADP−agarose chromatography used to determine the PAPS binding affinity because heparin and 3′,5′-ADP are the analogues of HS and PAPS, respectively. SDS−PAGE followed by staining with Coomassie blue was used to determine the amount of b3-OST-1 and truncated b3-OST-1 that eluted from the affinity chromatographies using different concentrations of NaCl (Figure 5). As shown in Figure 5A, we detected

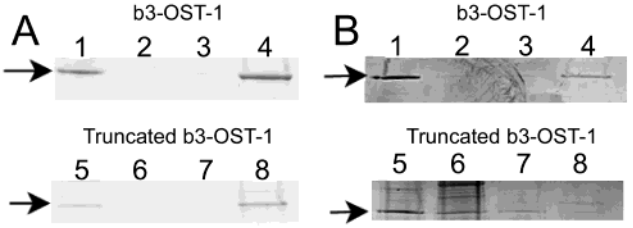

FIGURE 5: Analysis of the binding of b3-OST-1 and truncated b3-OST-1 to HS and PAPS. SDS−PAGE analysis of the fractions eluted from heparin−Sepharose (A) and 3′,5′-ADP−agaorse (B) chromatography fractions. Wild-type (b3-OST-1) fractions in panel A and B are the WT protein (lane 1), the unbound fraction (100 mM NaCl) (lane 2), the low-ionic strength elution fraction (250 mM NaCl) (lane 3), and the high-ionic strength elution fraction (1 M NaCl) (lane 4). Truncated b3-OST-1 fractions in panel A and B are truncated b3-OST-1 (lane 5), unbound fractions (100 mM NaCl) (lane 6), the low-ionic strength elution fraction (250 mM NaCl) (lane 7), and the high-ionic strength elution fraction (1 M NaCl) (lane 8). The arrows indicate the migrated position of the protein band for b3-OST-1 or truncated b3-OST-1 on SDS−PAGE.

both b3-OST-1 and truncated b3-OST-1 in the high-ionic strength elution fractions (1 M NaCl) from the heparin−Sepharose column. This suggests that the truncated b3-OST-1 and b3-OST-1 have similar affinity for HS (Figure 5A, lanes 4 and 8). In contrast, the majority of the truncated b3-OST-1 was eluted from 3′,5′-ADP chromatography at 100 mM (unbound fraction) and 250 mM NaCl (low-ionic strength elution fraction) (Figure 5B, lanes 6 and 7), whereas b3-OST-1 was only detected in the high-ionic strength elution fraction (1 M NaCl) (Figure 5B, lane 4). This suggests that the truncated b3-OST-1 has a decreased affinity for PAP and PAPS compared with the wild type. In conclusion, the loss of sulfotransferase activity in truncated b3-OST-1 is likely due to a decrease in the affinity for PAPS. Thus, we are unable to conclude that the conformational change is required for the enzymatic activity despite the fact that HS cannot induce a fluorescence increase for truncated b3-OST-1.

DISCUSSION

Heparan sulfate biosynthesis is a complex process that yields structurally diverse HS chains involved in an extensive array of physiological roles. HS sulfotransferases are responsible for introducing the structural diversity in HS chains; however, a complete understanding of the reaction mechanism of sulfotransferases remains elusive. The reaction mechanism has been studied extensively for NDST-1, and the HS and PAPS binding motifs have been identified (*21*, *34*). Nonetheless, the absence of a crystal structure for the ternary complex of NDST-1 with HS and PAPS precludes a full understanding of the interactions between the substrate and the enzyme. In this paper, we describe a conformational change that occurs in 3-OST-1 upon binding to HS. To our knowledge, such an observation has not been reported.

Two lines of evidence support the conclusion that a conformational change occurs in 3-OSTs upon binding to HS. First, we observed an increase in the fluorescence intensity at λ_{em} for 3-OSTs when bound to HS, which was only induced by binding to HS, but not CS. Fluorescence has been used to study the conformational changes that numerous proteins undergo upon binding their ligands (*35*,

36), including the binding of antithrombin (AT) to HS (*37*, *38*). The conformational change of AT was subsequently confirmed by X-ray crystallography of the AT and pentasaccharide complex (*39*). An increase in the intrinsic fluorescence of 3-OST-1 upon ligand binding could be attributed to a simple binding event. However, this premise cannot explain the observations made with the truncated b3-OST-1 mutant. The truncated mutant lacked the C-terminal region that participates in the conformational change as determined by differential chemical modification. This mutant (truncated b3-OST-1) was observed to have an affinity for HS similar to that of the wild-type protein (b3-OST-1) (Figure 5), suggesting that the binding of HS to truncated b3-OST-1 occurred. However, HS cannot induce a fluorescence increase for truncated b3-OST-1, as observed for wild-type 3-OSTs. Therefore, the increase in intrinsic fluorescence that was observed for the 3-OSTs does suggest that a conformational change may be occurring upon binding of HS.

Second, further investigation of the conformational change was completed using differential chemical modification of m3-OST-1. Determining the relative reactivity with respect to acetic anhydride allowed us to probe the solvent accessibility of lysine residues with and without HS bound. We observed that lysine residues in different regions of m3-OST-1 have distinct relative reactivity with respect to acetylation in the presence or absence of HS. While the binding of HS to 3-OST-1 has differential effects on the solvent accessibility of the lysine residues, the residues located in the C-terminal region of the protein showed a substantial increase in solvent accessibility when m3-OST-1 bound to HS. These observations suggest that the protein undergoes a conformational change.

To gain a better understanding of the role of the C-terminal domain plays in catalytic function, a homology model of m3-OST-1 was built using INSIGHT-II and NDST-1 was used as the template (*21*, *23*). The C-terminal region that exhibited an increase in solvent accessibility was mapped to the C-terminal α-helix, which is located on the opposite side of the proposed HS binding site (Figure 6). This α-helix is also located away from the PAPS binding site. This model suggests that the C-terminal domain is not directly involved in binding either HS or PAPS. However, deletion of this α-helix (truncated b3-OST-1) resulted in a 200-fold decrease in sulfotransferase activity. In addition, the increase in intrinsic fluorescence observed for the wild-type enzyme upon binding HS was greatly reduced for the truncated b3-OST-1. Taken together, these data suggest that these C-terminal amino acids are critical for both the conformational change, and catalysis. Further analysis of the truncated b3-OST-1 showed that the truncated b3-OST-1 has a similar affinity for HS but a decreased affinity for PAPS. This decrease in PAPS binding affinity was unexpected, as the model predicts this α-helix does not directly interact with PAPS. We noted that Gorokhov and colleagues predicted that the C-terminus of NDST-1 might be involved in binding to the 3′-phosphate of PAP, and two residues, K833 and R835, of NDST-1 are very close to the 3′-phosphate of PAP (*22*). The corresponding residues based on the sequence alignment in 3-OST-1 are K272 and R274 (*32*). The truncated b3-OST-1 described in this study includes both these residues, suggesting that the residues for binding the 3′-phosphate of PAP are present. A possible explanation for both the decreased affinity of truncated b3-OST-1 for PAPS and the observed substrate-induced conformational change is that this C-terminal α-helix region stabilizes the active conformation of 3-OST-1. Interestingly, Wei and Swiedler described a unique role for the C-terminal region of NDST-1 (*40*). They observed that the removal of as few as 15 amino acids from the C-terminus of NDST-1 resulted in a complete loss of both the sulfotransferase and deacetylase activity. It is known that the deacetylase activity of NDST does not require binding to PAPS (*41*). These data suggest a complex role for the C-terminal region of NDST-1 and 3-OST-1 in the catalytic functions of these enzymes.

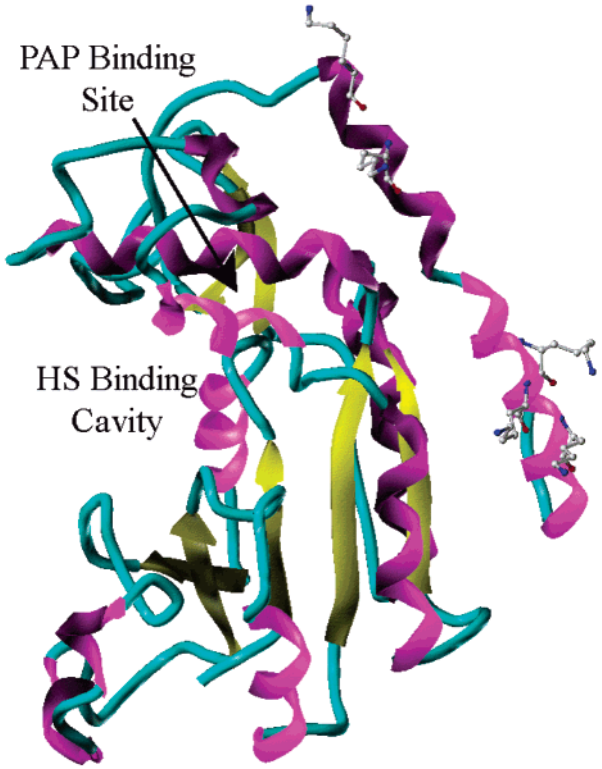

FIGURE 6: Homology model of m3-OST-1. The model is colored according to secondary structure. The lysine residues in the C-terminus that were observed to undergo a conformational change are represented with ball-and-stick illustrations. The potential PAP and HS binding sites are denoted with arrows.

A conformational change has not been reported for NDST-1 (*24*). Extensive computational simulation of the ternary complex of NDST-1, PAPS, and a disaccharide has not resulted in any observed major conformation changes (*22*). However, the study utilized a disaccharide, rather than a polysaccharide, as the acceptor substrate for NDST-1. The difference in the size and structural complexity between the disaccharide and polysaccharide could have a substantial impact on the conformation of the enzyme.

Conformational changes have been observed for numerous HS binding proteins, such as antithrombin (*42*), microtubule-associated protein Tau (*43*), and hepatocyte growth factor/scatter factor (*44*). Binding of HS induces a conformational change that is required for activity of those proteins. Our data suggest that HS induces a conformational change in 3-OSTs, and that this conformational change provides a potential new mechanism for understanding the activity of 3-OSTs and HS.

ACKNOWLEDGMENT

We thank Dr. Ashutosh Tripathy (Macromolecular Interaction Facility, University of North Carolina) for the assistance with the fluorescence experiments. We also thank Dr. Jinghua Chen (University of North Carolina) for providing us with the purified 3-OST-5 protein.

REFERENCES

1. Alexander, C. M., Reichsman, F., Hinkes, M. T., Lincecum, J., Becker, K. A., Cumberledge, S., and Bernfield, M. (2000) Syndecan-1 is required for Wnt-1-induced mammary tumorigenesis in mice, *Nat. Genet. 25*, 329−332.
2. Bernfield, M., Gotte, M., Park, P. W., Reizes, O., Fitzgerald, M. L., Lincecum, J., and Zako, M. (1999) Functions of cell surface heparan sulfate proteoglycans, *Annu. Rev. Biochem. 68*, 729−777.
3. Liu, J., and Thorp, S. C. (2002) Heparan sulfate and the roles in assisting viral infections, *Med. Res. Rev. 22*, 1−25.
4. Reizes, O., Lincecum, J., Wang, Z., Goldberger, O., Huang, L., Kaksonen, M., Ahima, R., Hinkes, M. T., Barsh, G. S., Rauvala, H., and Bernfield, M. (2001) Transgenic Expression of Syndecan-1 Uncovers a Physiological Control of Feeding Behavior by Syndecan-3, *Cell 106*, 105−116.
5. Rosenberg, R. D., Showrak, N. W., Liu, J., Schwartz, J. J., and Zhang, L. (1997) Heparan sulfate proteoglycans of the cardiovascular system: specific structures emerge but how is synthesis regulated? *J. Clin. Invest. 99*, 2062−2070.
6. Sasisekharan, R., Shriver, Z., Venkataraman, G., and Narayanasami, U. (2002) Roles of heparin-sulphate glycosaminoglycans in cancer, *Nat. Rev. Cancer 2*, 521−528.
7. Lindahl, U., Kusche-Gullberg, M., and Kjellen, L. (1998) Regulated diversity of heparan sulfate, *J. Biol. Chem. 273*, 24979−24982.
8. Aikawa, J.-i., Grobe, K., Tsujimoto, M., and Esko, J. D. (2001) Multiple isozymes of heparan sulfates/heparin GlcNAc N-deacetylase/GlcN N-sulfotransferase: Structure and activity of the fourth member, NDST4, *J. Biol. Chem. 276*, 5876−5882.
9. Habuchi, H., Tanaka, M., Habuchi, O., Yoshida, K., Suzuki, H., Ban, K., and Kimata, K. (2000) The occurrence of three isoforms of heparan sulfate 6-O-sulfotransferase having different specificities for hexuronic acid adjacent to the targeted N-sulfoglucosamine, *J. Biol. Chem. 275*, 2859−2868.
10. Liu, J., and Rosenberg, R. D. (2002) in *Handbook of glycosyltransferases and their related genes* (Taniguchi, N., and Fukuda, M., Eds.) pp 475−483, Springer-Verlag, Tokyo.
11. Liu, J., Shworak, N. W., Sinaÿ, P., Schwartz, J. J., Zhang, L., Fritze, L. M. S., and Rosenberg, R. D. (1999) Expression of heparan sulfate D-glucosaminyl 3-*O*-sulfotransferase isoforms reveals novel substrate specificities, *J. Biol. Chem. 274*, 5185−5192.
12. Xia, G., Chen, J., Tiwari, V., Ju, W., Li, J.-P., Malmström, A., Shukla, D., and Liu, J. (2002) Heparan sulfate 3-O-sulfotransferase isoform 5 generates both an antithrombin-binding site and an entry receptor for herpes simplex virus, type 1, *J. Biol. Chem. 277*, 37912−37919.
13. Jemth, P., Smeds, E., Do, A.-T., Habuchi, H., Kimata, K., Lindahl, U., and Kusche-Gullberg, M. (2003) Oligosaccharide library-based assessment of heparan sulfate 6-O-sulfotransfer substrate specificity, *J. Biol. Chem. 278*, 24371−24376.
14. Smeds, E., Habuchi, H., Do, A.-T., Hjertson, E., Grundberg, H., Kimata, K., Lindahl, U., and Kusche-Gullberg, M. (2003) Substrate specificities of mouse heparan sulphate glucosaminyl 6-O-sulfotransferases, *Biochem. J. 372* (Part 2), 371−380.
15. Liu, J., Shworak, N. W., Fritze, L. M. S., Edelberg, J. M., and Rosenberg, R. D. (1996) Purification of heparan sulfate D-glucosaminyl 3-*O*-sulfotransferase, *J. Biol. Chem. 271*, 27072−27082.
16. McKeehan, W. L., Wu, X., and Kan, M. (1999) Requirement for anticoagulant heparan sulfate in the fibroblast growth factor receptor complex, *J. Biol. Chem. 274*, 21511−21514.
17. Shukla, D., Liu, J., Blaiklock, P., Shworak, N. W., Bai, X., Esko, J. D., Cohen, G. H., Eisenberg, R. J., Rosenberg, R. D., and Spear, P. G. (1999) A novel role for 3-O-sulfated heparan sulfate in herpes simplex virus 1 entry, *Cell 99*, 13−22.
18. Ye, S., Luo, Y., Lu, W., Jones, R. B., Linhardt, R. J., Capila, I., Toida, T., Kan, M., Pelletier, H., and McKeehan, W. L. (2001) Structural basis for interaction of FGF-1, FGF-2, and FGF-7 with different heparan sulfate motifs, *Biochemistry 40*, 14429−14439.
19. Borjigin, J., Deng, J., Sun, X., Jesus, M., Liu, T., and Wang, M. W. (2003) Diurnal pineal 3-O-sulphotransferase 2 expression controlled by β-andrenergic repression, *J. Biol. Chem. 278*, 16315−16319.
20. Miyamoto, K., Asada, K., Fukutomi, T., Okochi, E., Yagi, Y., Hasegawa, T., Asahara, T., Sugimura, T., and Ushijima, T. (2003) Methylation-associated silencing of heparan sulfate D-glucosaminyl 3-O-sulfotransferase-2 (3-OST-2) in human breast, colon, lung and pancreatic cancers, *Oncogene 22*, 274−280.
21. Kakuta, Y., Sueyoshi, T., Negishi, M., and Pedersen, L. C. (1999) Crystal structure of the sulfotransferase domain of human heparan sulfate N-deacetylase/N-sulfotransferase 1, *J. Biol. Chem. 274*, 10673−10676.
22. Gorokhov, A., Perera, L., Darden, T. A., Negishi, M., Pedersen, L. C., and Pedersen, L. G. (2000) Heparan sulfate biosynthesis: A theoretical study of the initial sulfation step by N-deacetylase/N-sulfotransferase, *Biophys. J. 79*, 2909−2917.
23. Raman, R., Myette, J., Venkataraman, G., Sasisekharan, V., and Sasisekharan, R. (2002) Identification of structural motifs and amino acids within the structure of human heparan sulfate 3-*O*-sulfotransferase that mediate enzymatic function, *Biochem. Biophys. Res. Commun. 290*, 1214−1219.
24. Negishi, M., Pedersen, L. G., Petrotchenko, E., Shevtsov, S., Gorokhov, A., Kakuta, Y., and Pedersen, L. C. (2001) Structures and functions of sulfotransferases, *Arch. Biochem. Biophys. 390*, 149−157.
25. Liu, J., Shriver, Z., Blaiklock, P., Yoshida, K., Sasisekharan, R., and Rosenberg, R. D. (1999) Heparan sulfate D-glucosaminyl 3-O-sulfotransferase-3A sulfates N-unsubstituted glucosamine residues, *J. Biol. Chem. 274*, 38155−38162.
26. Chen, J., Duncan, M. B., Carrick, K., Pope, M., and Liu, J. (2003) Biosynthesis of 3-O-sulfated heparan sulfate: unique substrate specificity of heparan sulfate 3-O-sulfotransferase isoform 5, *Glycobiology 13*, 785−794.
27. Hochleitner, E. O., Borchers, C., Parker, C., Bienstock, R. J., and Tomer, K. B. (2000) Characterization of a discontinuous epitope of the human immunodeficiency virus (HIV) core protein p24 by epitope excision and differential chemical modification followed by mass spectrometric peptide mapping analysis, *Protein Sci. 9*, 487−496.
28. Borchers, C., Peter, J. F., Hall, M. C., Kunkel, T. A., and Tomer, K. B. (2000) Identification of In-Gel Digested Proteins by Complementary Peptide-Mass Fingerprinting and Tandem Mass Spectrometry Data Obtained on an Electrospray Ionization Quadrupole Time-of-Flight Mass Spectrometer, *Anal. Chem. 72*, 1163−1168.
29. Shworak, N. W., Liu, J., Fritze, L. M. S., Schwartz, J. J., Zhang, L., Logeart, D., and Rosenberg, R. D. (1997) Molecular cloning and expression of mouse and human cDNAs encoding heparan sulfate D-glucosaminyl 3-*O*-sulfotransferase, *J. Biol. Chem. 272*, 28008−28019.
30. Fiedler, W., Borchers, C., Macht, M., Deininger, S. O., and Przybylski, M. (1998) Molecular characterization of a conformational epitope of hen egg white lysozyme by differential chemical modification of immune complexes and mass spectrometric peptide mapping, *Bioconjugate Chem. 9*, 236−241.
31. Vilbois, F., Caspers, P., da Prada, M., Lang, G., Karrer, C., Lahm, H. W., and Cesura, A. M. (1994) Mass spectrometric analysis of human soluble catechol O-methyltransferase expressed in *Escherichia coli*. Identification of a product of ribosomal frameshifting and of reactive cysteines involved in S-adenosyl-L-methionine binding, *Eur. J. Biochem. 222*, 377−386.
32. Shworak, N. W., Liu, J., Petros, L. M., Zhang, L., Kobayashi, M., Copeland, N. G., Jenkins, N. A., and Rosenberg, R. D. (1999) Diversity of the extensive heparan sulfate D-glucosaminyl 3-*O*-sulfotransferase (3-OST) multigene family, *J. Biol. Chem. 274*, 5170−5184.
33. Marsolais, F., Laviolette, M., Kakuta, Y., Negishi, M., Pedersen, L., Auger, M., and Varin, L. (1999) 3′-Phosphoadenosine 5′-phosphosulfate binding site of flavonol 3-sulfotransferase studied by affinity chromatography and ^{31}P NMR, *Biochemistry 38*, 4066−4071.
34. Kakuta, Y., Li, L., Pedersen, L. C., Pedersen, L. G., and Negishi, M. (2003) Heparan sulphate N-sulphotransferase activity: reaction

mechanism and substrate recognition, *Biochem. Soc. Trans. 31* (Part 2), 331−334.
35. Harris, D. A., Rueda, D., and Walter, N. G. (2002) Local conformational changes in the catalytic core of the trans-acting hepatitis delta virus ribozyme accompany catalysis, *Biochemistry 41*, 12051−12061.
36. Lacapere, J. J., Boulla, G., Lund, F. E., Primack, J., Oppenheimer, N., Schuber, F., and Deterre, P. (2003) Fluorometric studies of ligand-induced conformational changes of CD38, *Biochim. Biophys. Acta 1652*, 17−26.
37. Futamura, A., Beechem, J. M., and Gettins, P. G. (2001) Conformational equilibrium of the reactive center loop of antithrombin examined by steady state and time-resolved fluorescence measurements: consequences for the mechanism of factor Xa inhibition by antithrombin-heparin complexes, *Biochemistry 40*, 6680−6687.
38. Meagher, J. L., Beechem, J. M., Olson, S. T., and Gettins, P. G. (1998) Deconvolution of the fluorescence emission spectrum of human antithrombin and identification of the tryptophan residues that are responsive to heparin binding, *J. Biol. Chem. 273*, 23283−23289.
39. Skinner, R., Chang, W.-S. W., Jin, L., Pei, X., Huntington, J. A., Abrahams, J.-P., Carrell, R. W., and Lomas, D. A. (1998) Implications for function and therapy of a 2.9 Å structure of binary-complexed antithrombin, *J. Mol. Biol. 283*, 9−14.
40. Wei, Z., and Swiedler, S. J. (1999) Functional analysis of conserved cysteines in heparan sulfate N-deacetylase-N-sulfotransferases, *J. Biol. Chem. 274*, 1966−1970.
41. Bengtsson, J., Eriksson, I., and Kjellen, L. (2003) Distinct effects on heparan sulfate structure by different active site mutations in NDST-1, *Biochemistry 42*, 2110−2115.
42. Jin, L., Abrahams, P., Skinner, R., Petitou, M., Pike, R. N., and Carrell, R. W. (1997) The anticoagulant activation of antithrombin by heparin, *Proc. Natl. Acad. Sci. U.S.A. 94*, 14683−14688.
43. Paudel, H. K., and Li, W. (1999) Heparin-induced conformational change in microtubule-associated protein tau as detected by chemical cross-linking and phosphopeptide mapping, *J. Biol. Chem. 274*, 8029−8038.
44. Lyon, M., Deakin, J. A., and Gallagher, J. T. (2002) The mode of action of heparan and dermatan sulfates in the regulation of hepatocyte growth factor/scatter factor, *J. Biol. Chem. 277*, 1040−1046.

BI0499112